Robust Mølmer-Sørensen gate for neutral atoms using rapid adiabatic Rydberg dressing

Anupam Mitra,[1,2,*] Michael J. Martin,[3,4] Grant W. Biedermann,[1,4,5] Alberto M. Marino,[5,4]
Pablo M. Poggi,[1,2] and Ivan H. Deutsch[1,2,†]

[1]*Center for Quantum Information and Control, University of New Mexico, Albuquerque, New Mexico 87131, USA*
[2]*Department of Physics and Astronomy, University of New Mexico, Albuquerque, New Mexico 87106, USA*
[3]*Los Alamos National Laboratory, Los Alamos, New Mexico 87545, USA*
[4]*Sandia National Laboratories, Albuquerque, New Mexico 87123, USA*
[5]*Department of Physics and Astronomy, University of Oklahoma, Norman, Oklahoma 73019, USA*

The Rydberg blockade mechanism is now routinely considered for entangling qubits encoded in clock states of neutral atoms. Challenges towards implementing entangling gates with high fidelity include errors due to thermal motion of atoms, laser amplitude inhomogeneities, and imperfect Rydberg blockade. We show that adiabatic rapid passage by Rydberg dressing provides a mechanism for implementing two-qubit entangling gates by accumulating phases that are robust to these imperfections. We find that the typical error in implementing a two-qubit gate, such as the controlled phase gate, is dominated by errors in the single-atom light shift, and that this can be easily corrected using adiabatic dressing interleaved with a simple spin echo sequence. This results in a two-qubit Mølmer-Sørensen gate. A gate fidelity ~ 0.995 is achievable with modest experimental parameters and a path to higher fidelities is possible for Rydberg states in atoms with a stronger blockade, longer lifetimes, and larger Rabi frequencies.

Arrays of trapped neutral atoms interacting via the electric dipole-dipole interaction (EDDI) have emerged as a potential scalable platform for quantum computing [1–3]. Near term applications include simulation of Ising models [4,5] and optimization [6–8]. In the longer term, this system is a promising platform for universal fault-tolerant quantum computing given long-lived qubits at the heart of ultraprecise atomic clocks [9] and flexible trapping geometries [10–13]. High fidelity, on demand one-qubit gates have been demonstrated [14,15] but the implementation of two-qubit gates with the fidelities required for fault tolerance remains a critical challenge.

Entangling gates based on the EDDI Rydberg-blockade mechanism [16–19] were first demonstrated in seminal experiments [20,21]. In recent developments, high-fidelity entangling interactions of qubits encoded in ground and Rydberg states [22] have been applied in a variety of applications [23–25], and the controlled-Z (CZ) gate on clock-state qubits have been demonstrated with a fidelity ~ 0.97 in 1D [26] and ~ 0.89 in 2D [27] arrays.

To achieve higher fidelity two-qubit entangling gates, we consider dressing clock states with Rydberg states via adiabatic rapid passage, a powerful tool for robust control [28]. Rydberg dressing has been studied for application in simulation [29–31] and metrology [6,32–36]. We have employed strong Rydberg dressing to create two-qubit entangled states [37], measured the light shifts of the adiabatically dressed entangled states [38], and showed how adiabatic dressing can be employed to implement a CZ gate with the potential for

Doppler-free excitation [39]. Adiabatic passage has also been studied in a variety of protocols as a mechanism for achieving entangling gates with the Rydberg blockade mechanism [40–45].

In the current work we extend our analysis and show how adiabatic passage to implement Rydberg dressing facilitates a method for realizing a Mølmer-Sørensen (MS) gate [46,47], with intrinsic robustness to a wide variety of imperfections. These include inhomogeneities in intensity and in detuning, such as those arising from Doppler shifts at finite temperature and Stark shifts from stray electric fields. As we will show, the dominant effect of such inhomogeneities is the errors incurred by the single-atom light shifts, which can be removed using a simple spin echo. Moreover, we can achieve adiabatic rapid passage such that the integrated time spent in the Rydberg state is on the same order as that for the standard pulsed protocol of Jaksch *et al.* [48] with equivalent Rabi frequencies, thereby maintaining a similar budget in the error due to finite Rydberg radiative lifetime. Gate fidelities ~ 0.995 are compatible with the typical inhomogeneities in current experiments and Rydberg state lifetimes $t \sim 100\ \mu s$. Longer-lived Rydberg states can facilitate better control of adiabatic passage to push fidelities even higher.

For generality, we consider an atom with two long-lived clock states to serve as the qubit states $|0\rangle$ and $|1\rangle$. These could be the hyperfine clock states of alkali atoms separated by a microwave frequency (e.g., Cs or Rb) [19], or the optical clock states of alkaline-earth-like atoms (e.g., Sr or Yb) [33,49,50]. The clock state $|1\rangle$ is optically coupled to a high-lying Rydberg state $|r\rangle$. The fundamental Hamiltonian governing the Rydberg gate between two atoms is $\hat{H}_{2\,\mathrm{atom}} = \hat{H}_\alpha + \hat{H}_\beta + V_{\mathrm{DD}}|rr\rangle\langle rr|$ where V_{DD} is the electric dipole interaction. $\hat{H}_\alpha$

$(\hat{H}_\beta)$ is the Hamiltonian for the atom α (β) coupled to the Rydberg laser,

$$\hat{H}_\alpha = \frac{1}{2m}\hat{p}_\alpha^2 - \Delta_{1r}|r\rangle_\alpha\langle r|_\alpha + \frac{1}{2}\Omega_{1r}\left(e^{ik_r\hat{z}_\alpha}|r\rangle_\alpha\langle 1|_\alpha + \text{H.c.}\right),$$

$$(1)$$

where Ω_{1r} and Δ_{1r} are the Rydberg laser Rabi frequency and detuning, respectively (here and throughout we set $\hbar = 1$), $\hat{p}_\alpha$ is the atomic momentum operator, and $\hat{z}_\alpha$ is the atomic position operator in the direction of the Rydberg laser. Ideally, the atoms are illuminated uniformly and see the same Rydberg laser intensity and detuning. Under those conditions it is natural to consider the basis of "bright" $|b\rangle = (e^{ik_1z_\beta}|1r\rangle + e^{ik_1z_\alpha}|r1\rangle)/\sqrt{2}$ and "dark" $|d\rangle = (e^{ik_1z_\beta}|1r\rangle - e^{ik_1z_\alpha}|r1\rangle)/\sqrt{2}$ states (here and throughout we use the abbreviated notation, $|xy\rangle = |x\rangle_\alpha|y\rangle_\beta$). We consider Rydberg interactions for atoms released from a trap, as is typically done in experiments, and treat the motion as that of a free particle, and the strong blockade regime $V_{DD} \gg \Omega_{1r}$ and neglect to zeroth order any population in the doubly excited Rydberg state $|rr\rangle$; corrections will be considered below. In the case of "frozen" atoms with zero momentum, the two-atom Hamiltonian takes the form [30,39]

$$\hat{H}_{2\,\text{atom}} = -\Delta_{1r}(|b\rangle\langle b| + |d\rangle\langle d|) + \frac{\sqrt{2}\Omega_{1r}}{2}(|b\rangle\langle 11| + \text{H.c.}).$$

$$(2)$$

A π rotation on the $|11\rangle \rightarrow |b\rangle$ transition yields an entangled state, recently achieved with fidelity 97% [22]. When there is thermal motion, the relative phase $e^{ik_{1r}(z_\beta - z_\alpha)}$ will vary, leading to coupling between bright and dark states, which limits the transfer of the entanglement from the bright state to the long-lived ground state qubits [20,27].

The dressed states of the zero-momentum two-atom Hamiltonian are [39]

$$|\widetilde{11}\rangle = \cos\frac{\theta_2}{2}|11\rangle + \sin\frac{\theta_2}{2}|b\rangle,$$

$$(3)$$

$$|\widetilde{b}\rangle = \cos\frac{\theta_2}{2}|b\rangle - \sin\frac{\theta_2}{2}|11\rangle,$$

$$(4)$$

where $\tan\theta_2 = -\sqrt{2}\Omega_{1r}/\Delta_{1r}$. In the dressed states, some character of the entangled bright state $|b\rangle$ is admixed with the ground state $|11\rangle$. The two-atom light shift of the ground state, mediated by the Rydberg blockade, is a shift in the energy eigenvalues of the dressed states with respect to the bare states, which under the perfect blockade approximation is $E_{LS}^{(2)} = \frac{1}{2}(-\Delta_{1r} \pm \sqrt{2\Omega_{1r}^2 + \Delta_{1r}^2})$ [30,37–39]. In the absence of the EDDI the light shift of this state is equal to twice the single-atom shift, $2E_{LS}^{(1)}$. The difference between the interacting and noninteracting shifts is the *entangling energy* κ [37–39],

$$\kappa = E_{LS}^{(2)} - 2E_{LS}^{(1)}$$

$$= \frac{1}{2}\left[\Delta_{1r} \pm \left(\sqrt{2\Omega_{1r}^2 + \Delta_{1r}^2} - 2\sqrt{\Omega_{1r}^2 + \Delta_{1r}^2}\right)\right]. \quad (5)$$

On resonance $\kappa \approx \pm 0.29\Omega_{1r}$, where $\Omega_{1r}/2\pi$ can be as large as a few MHz. For weak dressing, $|\Delta_{1r}| \gg \Omega_{1r}$, $\kappa \approx -\Omega_{1r}^4/8\Delta_{1r}^3$, which will generally be smaller than the rate of
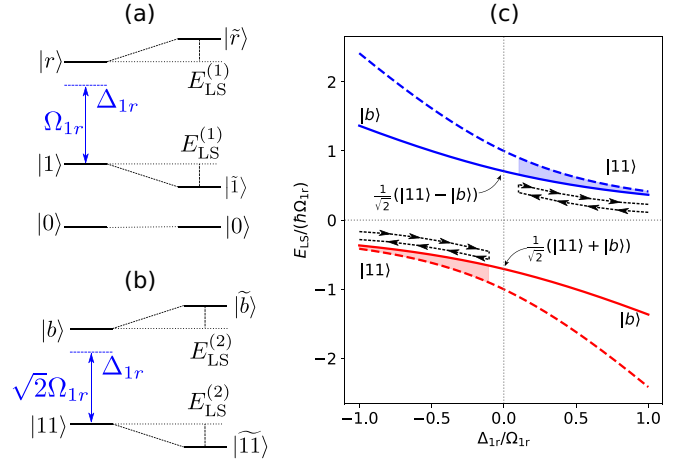

FIG. 1. (a) Qubit encoded into atomic clock states with the upper clock state, $|1\rangle$, coupled to a Rydberg state $|r\rangle$ with a Rabi frequency Ω_{1r} and detuning Δ_{1r}. (b) The two-atom state $|11\rangle$ is coupled to the entangled bright state $|b\rangle = (|1r\rangle + e^{i\varphi}|r1\rangle)/\sqrt{2}$ with Rabi frequency $\sqrt{2}\Omega_{1r}$. (c) Light shift of the state $|11\rangle$ as a function detuning. The dashed lines show the light shift in the absence of EDDI (top: starting from blue detuning; bottom: starting from red detuning), in an adiabatic passage to the doubly excited Rydberg state $|rr\rangle$. The solid lines show the light shift in the presence of EDDI under the perfect blockade approximation (top: starting from blue detuning; bottom: starting from red detuning). The shaded region shows the value of κ [Eq. (5)]. The dotted lines with arrows show examples of adiabatic passages used in our ramps (Fig. 2) to obtain entanglement in the ground state.

photon scattering, which scales as $1/\Delta_{1r}^2$. Thus weak dressing will not yield high-fidelity entangling gates in our protocol.

The dressed energy levels provide an adiabatic passage from the one-atom ground state $|1\rangle$ to the one-atom Rydberg state $|r\rangle$ and from the two-atom ground state $|11\rangle$ to the two-atom entangled bright state $|b\rangle$, as shown in Fig. 1(c). Assuming adiabatic evolution, we consider sweeping the detuning from $|11\rangle$ toward $|b\rangle$ and then back to $|11\rangle$, yielding an entangling phase given by $\vartheta_2 = \int \kappa \, dt$. While κ grows monotonically as we pass adiabatically from $|11\rangle$ to $|b\rangle$, the simultaneous restrictions of maintaining adiabaticity and limiting the phase ϑ_2 to the target value puts a constraint on the value of the final detuning. Operationally this final detuning is near resonance in our protocol, yielding the minimum gate time such that we simultaneously remain adiabatic but act fast compared to the decoherence rates.

To understand the general class of gates enabled by the phases accumulated in adiabatic evolution and their sensitivity to errors, we consider the Hamiltonian in the dressed qubit (DQ) ground subspace $\{|00\rangle, |0\tilde{1}\rangle, |\tilde{1}0\rangle, |\widetilde{11}\rangle\}$, where $|\tilde{1}\rangle$ is the one-atom dressed ground state that is a superposition of $|1\rangle$ and $|r\rangle$ with dressing angle given by $\tan\theta_1 = -\Omega_{1r}/\Delta_{1r}$. Let $\hat{\sigma}_z = |\tilde{1}\rangle\langle\tilde{1}| - |0\rangle\langle 0|$ be the adiabatic Pauli operator on one atom and $\hat{S}_z = \mathbb{1} \otimes \hat{\sigma}_z/2 + \hat{\sigma}_z/2 \otimes \mathbb{1}$ be the collective angular momentum operator. In the dressed atomic basis, the Hamiltonian in the ground subspace can be written as

$$\hat{H}_{DQ} = -\left(E_{LS}^{(1)} + \frac{\kappa}{2}\right)\hat{S}_z + \kappa\frac{\hat{S}_z^2}{2}.$$

$$(6)$$

This Hamiltonian generates symmetric, one-axis, two-qubit unitary transformations. The $\hat{S}_z$ term generates $\mathbb{SU}(2)$ rotations on the collective spin, while the $\hat{S}_z^2$ term "twists" the collective spin and also generates two-qubit entanglement. The quantization axis can be changed to any axis μ using additional global $\mathbb{SU}(2)$ rotations.

Consider, thus, the unitary transformation of the dressed qubits generated by adiabatic evolution with this Hamiltonian,

$$\hat{U}_\kappa = \exp\left(-i\vartheta_1\hat{S}_\mu - i\vartheta_2\frac{\hat{S}_\mu^2}{2}\right), \qquad (7)$$

where $\vartheta_1 = -\int\left(E_{\mathrm{LS}}^{(1)} + \frac{\kappa}{2}\right)dt$ is the rotation angle generated by the linear term, and $\vartheta_2 = \int\kappa\,dt$ is the twist angle generated by the quadratic term in the Hamiltonian. When the twist angle $\vartheta_2 = \pm\pi$, these gates are perfect entanglers [51], meaning that the gates can take a product state to a maximally entangled state. Examples of perfect entanglers of this kind are the CZ gate ($\mu = z$, $\vartheta_1 = \mp\pi/2$, $\vartheta_2 = \pm\pi$) and the MS gate ($\mu = x$, $\vartheta_1 = 0$, $\vartheta_2 = \pi$). A CZ gate is achieved by removing the phases accumulated due to the independent one-atom light shifts $E_{\mathrm{LS}}^{(1)}$ [39]. In contrast, the MS gate is achieved by removing *all* single-qubit phases contributing to ϑ_1. While theoretically this difference is trivial, the dominant source of gate infidelity is errors in ϑ_1, making the MS gate more robust than the CZ gate, as we will see below.

To implement a two-qubit gate of the form Eq. (7) we consider an adiabatic ramp in which we sweep both the Rabi frequency Ω_{1r} and detuning Δ_{1r} to dress ground states with Rydberg character and then undress them. This implements a rapid adiabatic passage of the logical $|11\rangle$ state to a near equal superposition of $|11\rangle$ and the entangled bright state $|b\rangle$. For a short time we hold the system in this superposition and then perform rapid adiabatic passage back to $|11\rangle$. All other logical states involve only single-atom dressing or no dressing. As an example, we consider an adiabatic schedule of dressing through a Gaussian ramp of Ω_{1r} and a linear ramp of the detuning Δ_{1r} according to

$$|\Delta_{1r}(t)| = \Delta_{\max} + \frac{(\Delta_{\max} - \Delta_{\min})}{(t_2 - t_1)}(t - t_1), \qquad (8)$$

$$\Omega_{1r}(t) = \Omega_{\min} + (\Omega_{\max} - \Omega_{\min})\exp\left(-\frac{(t - t_2)^2}{2t_w^2}\right). \qquad (9)$$

After a constant period, we reverse the ramp as shown in Fig. 2. The ramp is optimized to achieve a particular value of ϑ_2.

To implement the MS gate, we consider two adiabatic ramps, each achieving an entangling phase of $\vartheta_2 = \pm\pi/2$, with an echo pulse on the qubit transition, $\exp(-i\pi\hat{S}_x)$, between them [52]. The echo pulse cancels the ϑ_1 accumulated in the two adiabatic ramps, thus implementing a MS gate about the z axis. We convert this to a MS gate about the y axis using $\pi/2$ rotations about the x axis. An advantage of using these adiabatic ramps is they can be designed for any value of ϑ_2, not just integer multiples of π as in the pulse sequence $\pi_c - 2\pi_t - \pi_c$ on control (c) and target (t) qubits, proposed in the seminal work of Jaksch *et al.* [48]. The duration of this ramp, implementing $\vartheta_2 = \pi/2$, shown in Fig. 2 is $\approx 8.4 \times 2\pi/\Omega_{\max}$. We calculate the time spent in Rydberg states as the integrated time weighted by the Rydberg
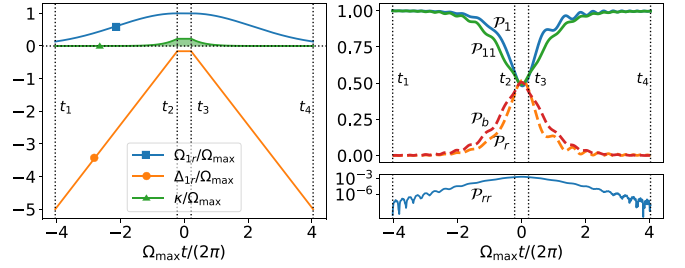

FIG. 2. Adiabatic ramp to implement a unitary transformation in Eq. (7) with $\vartheta_2 = \pi/2$, involving dressing from time t_1 to t_2, holding the parameters constant for a short interval t_2 to t_3, and undressing from t_3 to t_4. Left: Rabi frequency (blue, square); detuning (orange, circle), with a minimum value of $\Delta_{\min}/\Omega_{\max} \approx 0.1$; and entangling energy (green, triangle) as functions of time during the ramp, with a maximum value of $\kappa_{\max}/\Omega_{\max} \approx 0.25$. Right top: Population of $|01\rangle$ and $|10\rangle$ ($\mathcal{P}_1$, blue); population of $|0r\rangle$ and $|r0\rangle$ ($\mathcal{P}_r$ orange, dotted); population of $|11\rangle$ ($\mathcal{P}_{11}$, green); and population of $|b\rangle$ ($\mathcal{P}_b$, red, dotted). Right bottom: Population of $|rr\rangle$ ($\mathcal{P}_{rr}$) in a logarithmic scale.

population, $t_r = \int dt'\mathcal{P}_r(t')$. We find $t_r \approx 0.7 \times 2\pi/\Omega_{\max}$ for initial states $|01\rangle$ and $|10\rangle$ and $t_r \approx 0.9 \times 2\pi/\Omega_{\max}$ for initial state $|11\rangle$. As long as the Rabi period $2\pi/\Omega_{\max}$ is much larger than the radiative lifetime of the Rydberg states, these ramps are rapid and have small loss due to Rydberg state decay. Starting in $|11\rangle$ leads to time spent in the doubly excited Rydberg state $|rr\rangle$ of $0.0029 \times 2\pi/\Omega_{\max}$ when the EDDI is modest, e.g., $V_{\mathrm{DD}} = 10\,\Omega_{\max}$ for $\Omega_{\max}$ of a few MHz. The population dynamics, during the ramp are shown in Fig. 2.

We assess the performance of the gate by considering the fidelity between the implemented two-qubit gate $\hat{U}$ and the target ideal unitary transformation $\hat{V}$ defined using a normalized Hilbert Schmidt inner product between them, $\mathcal{F} = |\mathrm{tr}(\hat{U}\hat{V}^\dagger)|^2/16$, which estimates how well any input basis is mapped to the corresponding target output basis, by the implemented unitary [53]. In particular, we consider errors that can arise from inhomogeneities or coherent errors in the accumulated phases. The fidelity depends on the difference between twist angles $\delta\vartheta_2$ and the difference between rotation angles $\delta\vartheta_1$ of the implemented and target unitary maps according to

$$\mathcal{F} = \frac{1}{4}\left[1 + \cos^2(\delta\vartheta_1) + 2\cos(\delta\vartheta_1)\cos\left(\frac{\delta\vartheta_2}{2}\right)\right]. \qquad (10)$$

Importantly, the fidelity is much more sensitive to $\delta\vartheta_1$ than it is to $\delta\vartheta_2$. The twist angle ϑ_2 depends solely on the entangling energy κ. As this is the *difference* of two light shifts, it has some common mode cancellation of errors in the light shifts, while ϑ_1 has a contribution from independent single-atom light shifts with no such cancellation. This effect is seen in Fig. 3 which shows the fidelity plotted as a function of $\delta\vartheta_1$ when $\delta\vartheta_2 = 0$, that is, $\mathcal{F} = \frac{1}{2}[1 + \cos(\delta\vartheta_2/2)]$ and as a function of $\delta\vartheta_2$ when $\delta\vartheta_1 = 0$, that is, $\mathcal{F} = \frac{1}{4}[1 + \cos(\delta\vartheta_1)]^2$. Note, the CZ gate studied in [39] required knowledge of $E_{\mathrm{LS}}^{(1)}$ to remove the single-atom contribution to the phase, and errors will contribute substantially to infidelity through $\delta\vartheta_1$. In contrast, the MS gate is substantially less sensitive to such errors, as $\delta\vartheta_1$ can be made zero by using a spin echo [52].
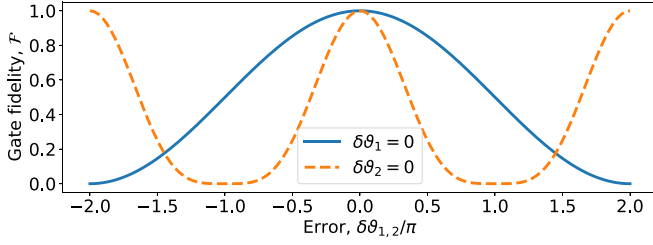
FIG. 3. Fidelity between a target and implemented unitary transformation, each of the forms given in Eq. (7), as a function of the error in the single-qubit rotation angle $\delta\vartheta_1$ (blue, solid line) and as a function of the error in the two-qubit twist angle $\delta\vartheta_2$ (orange, dotted line). The implementation of the CZ gate is very sensitive to errors caused by inhomogeneities, as it is dominated by $\delta\vartheta_1$ (orange, dotted line). In contrast, the MS gate is more robust, as it is prone to only errors in $\delta\vartheta_2$ (blue, solid line).

Let us consider the error channels and the intrinsic robustness of using adiabatic Rydberg dressing to implement the MS gate. Deleterious effects include thermal Doppler shifts and atomic motion in a spatially inhomogeneous exciting laser, imperfect blockade, and finite radiative lifetime of the Rydberg state. To see how this effect arises, let us revisit the dressed states, including the quantized motion. For generality we include quantized atomic momenta p_α and p_β of the two atoms in their Rydberg dressing interaction in addition to the electronic ground state and the bright and dark states. The bare states are the ground state $|G\rangle = |1, p_\alpha; 1, p_\beta\rangle$, bright state $|B\rangle = \frac{1}{\sqrt{2}}(|r, p_\alpha + k_{1r}; 1, p_\beta\rangle + |1, p_\alpha; r, p_\beta + k_{1r}\rangle)$, and dark state $|D\rangle = \frac{1}{\sqrt{2}}(|r, p_\alpha + k_{1r}; 1, p_\beta\rangle - |1, p_\alpha; r, p_\beta + k_{1r}\rangle)$. The two-atom Rydberg Hamiltonian now generalizes to [39]

$$
\begin{aligned}
\hat{H}_{2\,\text{atom}}(p_\alpha, p_\beta) = & -\left(\Delta_{1r} - \frac{k_{1r}P_{\text{CM}}}{M}\right)(|B\rangle\langle B| + |D\rangle\langle D|) \\
& + \left[V_{\text{DD}} - 2\left(\Delta_{1r} - \frac{k_{1r}P_{\text{CM}}}{M}\right)\right]|rr\rangle\langle rr| \\
& + \frac{k_{1r}p_{\text{rel}}}{m}(|B\rangle\langle D| + \text{H.c.}) + \frac{1}{2}\left(\frac{\Omega_\alpha + \Omega_\beta}{\sqrt{2}}\right) \\
& \times (|B\rangle\langle G| + |rr\rangle\langle B| + \text{H.c.}) \\
& + \frac{1}{2}\left(\frac{\Omega_\alpha - \Omega_\beta}{\sqrt{2}}\right)(|D\rangle\langle G| + |rr\rangle\langle D| + \text{H.c.}),
\end{aligned}
\tag{11}
$$

where $\Omega_\alpha = \Omega_{1r}(z_\alpha)$ and $\Omega_\beta = \Omega_{1r}(z_\beta)$ are the Rabi frequencies at the positions of atoms α and β; $P_{\text{CM}} = p_\alpha + p_\beta$ and $p_{\text{rel}} = (p_\alpha - p_\beta)/2$ are the center-of-mass and relative momenta of the atoms [39].

The standard protocol of Jaksch *et al.* [48] involves a pulse sequence on the control (c) and target (t) qubits, $\pi_c - 2\pi_t - \pi_c$, ideally yielding a CZ gate. In the presence of thermal atomic velocity v_c for the control atom, the transformation on the logical states is $|00\rangle \rightarrow |00\rangle$, $|01\rangle \rightarrow -|01\rangle$, $|10\rangle \rightarrow -e^{-ik_{1r}v_c\delta t}|10\rangle$, $|11\rangle \rightarrow -e^{-ik_{1r}v_c\delta t}|11\rangle$. Relative to the ideal CZ gate, there are additional phases due to the random Doppler shift acquired when the control atom stays in the Rydberg state for a time δt. For a thermal distribution of momenta, the

random distribution of phases cannot be compensated, which causes gate errors [20,22,26,27,39]. In contrast to the direct excitation to Rydberg states, for adiabatic Rydberg dressing, there are no random phases imparted to the qubits. Instead, the center-of-mass motion leads to a detuning error [39]. The relative motion leads to coupling between bright and dark states. However, while using an adiabatic ramp, this is suppressed due to the energy gap between the light-shifted bright state and unshifted dark state. The residual off-resonance $|\tilde{B}\rangle \leftrightarrow |D\rangle$ coupling leads to a small second order perturbative shift on the dressed ground state [39]. Moreover, a nonuniform intensity in which atoms see different Rabi frequencies can introduce a coupling between the ground $|11\rangle$ and the dark state $|D\rangle$, which gives a small perturbative shift on the dressed ground state.

Finally there is the effect of imperfect blockade. Whereas in the standard pulsed protocol this can be a major source of error, gates based on adiabatic dressing are more resilient to this effect. As long as the evolution is adiabatic, the dressed ground states will contain a small admixture of doubly excited Rydberg states in the superposition as shown in Fig. 2. This will affect the value of κ, but this can be measured, and the adiabatic ramp can be adjusted accordingly. If we are close to the blockade radius, the gradient of dressed ground state energy as a function of separation between the atoms will be small, and there will be negligible force on the atoms due to the EDDI. Of course nonadiabatic effects such as resonant excitation to other doubly excited Rydberg states can add additional errors, but these effects are not studied here.

As an example we consider ^{133}Cs as used in our experiment, with qubit states $|1\rangle = |6S_{1/2}, F = 4, m_F = 0\rangle$ and $|0\rangle = |6S_{1/2}, F = 3, m_F = 0\rangle$ [37,38], with $|1\rangle$ coupled through a one-photon transition at 319 nm (the "Rydberg laser") to state $|r\rangle = |64P_{3/2}, m_J = 3/2\rangle$. The qubit states can be connected with a microwave field or Raman laser fields. A maximum Rydberg Rabi frequency of $\Omega_{\text{max}}/2\pi = 4$ MHz, gives an entangling strength at our final detuning near resonance ($\Delta_{\text{min}} \approx 0.1\Omega_{\text{max}}$) of $\kappa/2\pi \approx 1$ MHz under the perfect blockade approximation. A contribution to detuning inhomogeneities arises from the width of atomic velocity distribution, $\propto \sqrt{k_B T/m}$ [20,27,54–56]. The width of the distribution of κ due to a thermal Doppler width of the atomic momenta distribution can be estimated as $\delta\kappa_{\text{th}} = k_{1r}\sqrt{\frac{k_B T}{m}}\sqrt{(\frac{\partial\kappa}{\partial\Delta_\alpha})^2 + (\frac{\partial\kappa}{\partial\Delta_\beta})^2}$, where $\Delta_\alpha = \Delta_{1r} - k_{1r}p_\alpha/m$ and similarly for Δ_β. For our experiment, an atomic temperature of 10 μK [38] corresponds to $k_{1r}\sqrt{k_B T/m} \approx 0.02\Omega_{\text{max}}$, therefore $\delta\kappa \sim 10^{-2}\Omega_{\text{max}}$, leading to $\delta\vartheta_2/\vartheta_2 \approx 4 \times 10^{-2}$ for the example parameters used here. The Rydberg laser uses a Gaussian beam with a waist of about 15 μm, the transverse atomic position spread is about 1.45 μm, and the atomic separation is about 2 μm. This gives us a Rabi frequency inhomogeneity of $\delta\Omega_{1r} \approx 0.01\Omega_{1r}$.

We model the experimental scenario by considering the detuning Δ_{1r} and Rabi frequency Ω_{1r} for each atom to be sampled from a normal distribution with mean equal to the fiducial value and standard deviation determined by the level of imperfections in the experiment. We simulate the implementation of the CZ gate using the protocol proposed earlier [39] and
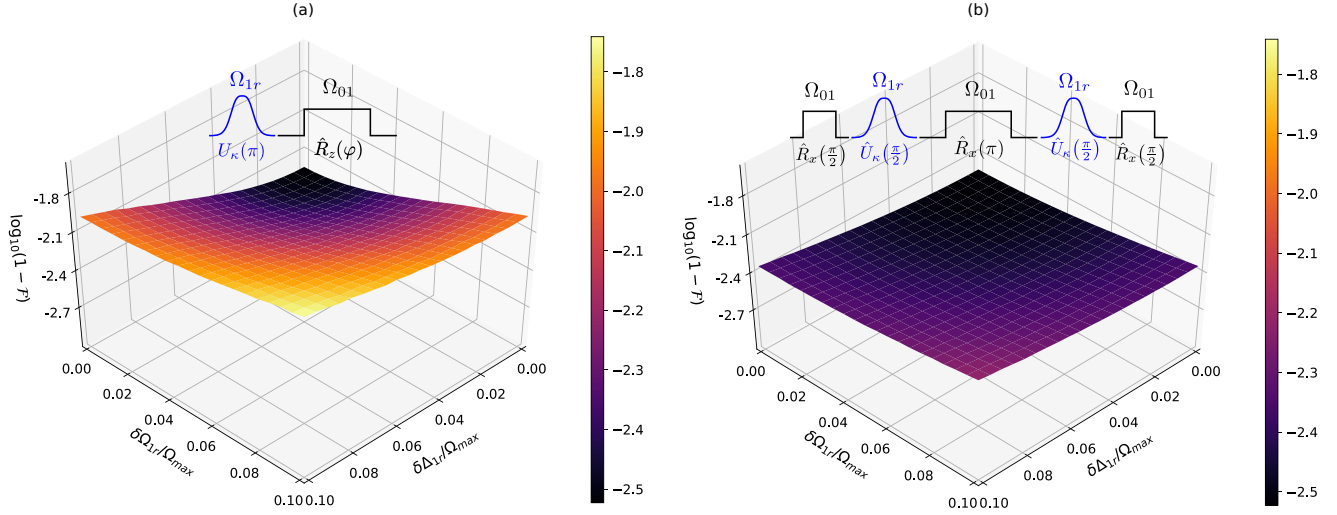
FIG. 4. (a) Top: Implementing the CZ gate as proposed in [39] using an adiabatic ramp, followed by removal of phases accumulated due to one-atom light shifts using a single-qubit rotation $\hat{R}_z(\varphi)$, where $\varphi = \int dt' E_{LS}^{(1)}(t')$. Bottom: Simulated infidelities of implementing the CZ gate with different levels of inhomogeneities in Δ_{1r} and Ω_{1r}. (b) Top: Implementing the MS gate as done in [52] using two adiabatic ramps, with a spin echo in between. Bottom: Simulated infidelities of implementing the MS gate with different levels of inhomogeneities in Δ_{1r} and Ω_{1r}.

the implementation of the MS gate using two adiabatic ramps and a spin echo, over a range of inhomogeneities $\delta\Delta_{1r}$ and $\delta\Omega_{1r}$. The gate fidelity including inhomogeneities, imperfect blockade, and Rydberg state decay [Rydberg lifetime $\tau_r \sim 10^3(2\pi/\Omega_{max})$] for an EDDI strength of $10\Omega_{max}$ and the target gate is shown in Fig. 4(a) for the CZ gate and Fig. 4(b) for the MS gate. As expected from Fig. 3, we see that implementing the MS gate using two adiabatic ramps and a spin echo is much more robust to inhomogeneities in Ω_{1r} and Δ_{1r} than implementing the CZ gate using an adiabatic ramp (Fig. 4). For example, when we increase the level of imperfections from 0 to about 10% of the maximum Rabi frequency Ω_{max} in the Rabi frequency and detuning, the MS gate fidelity falls from about 0.997 to about 0.995, while the CZ gate fidelity falls from about 0.997 to about 0.986. Therefore, high-fidelity gates are possible at room temperature with modest radiative lifetimes, consistent with the demands of adiabatic evolution.

Ultimately, the best achievable adiabaticity is limited by the finite radiative lifetime of the Rydberg states, which is the fundamental source of error [18,19] and limits the adiabaticity of the adiabatic ramp. The effective lifetime τ_r is due to contributions of different decay channels including ionization, spontaneous emission, and stimulated emission via coupling to blackbody radiation. The effect of finite radiative lifetime of the Rydberg state can be estimated by the quantity $\pi/(\kappa\tau_r)$ which compares how quickly atoms decay versus how quickly they accumulate entangling phase. The entangling phase is accumulated faster with a larger Rabi frequency, Ω_{1r}. More precisely, the time spent by atoms in the Rydberg state is quantified by the integrated Rydberg population, described above. Optimizing the parameters of the adiabatic ramp, we can satisfy $t_r/\tau_r \ll 1$ as long as $\Omega_{max}\tau_r \ll 1$. For example, for a lifetime of $\tau_r = 140\,\mu$s [22,57] and given $\kappa/2\pi \approx 1$ MHz, $\pi/(\kappa\tau_r) \sim 10^{-3}$. Lifetimes of a few milliseconds,

achievable by choosing higher lying Rydberg states and for cryogenic environments of a few kelvin [19] would give $\pi/(\kappa\tau_r) \sim 10^{-4}$.

In summary, adiabatic Rydberg dressing provides a robust method for harnessing the EDDI between Rydberg excited atoms to generate entanglement between qubits encoded in atomic clock states. We have shown that with current experimental capabilities, a two-qubit MS entangling gate with a fidelity of ~ 0.995 is within reach by interleaving of adiabatic Rydberg dressing and undressing with a spin echo on the qubit transition. Even higher fidelity gates are possible at cryogenic temperatures which substantially increases the Rydberg state lifetime. Such longer coherence times allow for improved adiabatic ramps and the potential use of more sophisticated robust control [58] to correct residual inhomogeneities not canceled in simple spin echo.

[1] G. K. Brennen, C. M. Caves, P. S. Jessen, and I. H. Deutsch, Phys. Rev. Lett. **82**, 1060 (1999).

[2] G. K. Brennen, I. H. Deutsch, and P. S. Jessen, Phys. Rev. A **61**, 062309 (2000).

[3] D. S. Weiss and M. Saffman, Phys. Today **70** (7), 44 (2017).

[4] H. Labuhn, D. Barredo, S. Ravets, S. De Léséleuc, T. Macrì, T. Lahaye, and A. Browaeys, Nature (London) **534**, 667 (2016).

[5] S. de Léséleuc, S. Weber, V. Lienhard, D. Barredo, H. P. Büchler, T. Lahaye, and A. Browaeys, Phys. Rev. Lett. **120**, 113602 (2018).

[6] T. Keating, K. Goyal, Y.-Y. Jau, G. W. Biedermann, A. J. Landahl, and I. H. Deutsch, Phys. Rev. A **87**, 052314 (2013).

[7] L. Zhou, S.-T. Wang, S. Choi, H. Pichler, and M. D. Lukin, arXiv:1812.01041.

[8] H. Pichler, S.-T. Wang, L. Zhou, S. Choi, and M. D. Lukin, arXiv:1809.04954.

[9] A. D. Ludlow, M. M. Boyd, J. Ye, E. Peik, and P. O. Schmidt, Rev. Mod. Phys. **87**, 637 (2015).

[10] M. Endres, H. Bernien, A. Keesling, H. Levine, E. R. Anschuetz, A. Krajenbrink, C. Senko, V. Vuletic, M. Greiner, and M. D. Lukin, Science **354**, 1024 (2016).

[11] D. Barredo, S. De Léséleuc, V. Lienhard, T. Lahaye, and A. Browaeys, Science **354**, 1021 (2016).

[12] D. Barredo, V. Lienhard, S. De Leseleuc, T. Lahaye, and A. Browaeys, Nature (London) **561**, 79 (2018).

[13] A. Kumar, T.-Y. Wu, F. Giraldo, and D. S. Weiss, Nature (London) **561**, 83 (2018).

[14] Y. Wang, X. Zhang, T. A. Corcovilos, A. Kumar, and D. S. Weiss, Phys. Rev. Lett. **115**, 043003 (2015).

[15] Y. Wang, A. Kumar, T.-Y. Wu, and D. S. Weiss, Science **352**, 1562 (2016).

[16] D. Jaksch, H.-J. Briegel, J.-I. Cirac, C.-W. Gardiner, and P. Zoller, Phys. Rev. Lett. **82**, 1975 (1999).

[17] M.-D. Lukin, M. Fleischhauer, R. Cote, L.-M. Duan, D. Jaksch, J. I. Cirac, and P. Zoller, Phys. Rev. Lett. **87**, 037901 (2001).

[18] M. Saffman, T. G. Walker, and K. Mølmer, Rev. Mod. Phys. **82**, 2313 (2010).

[19] M. Saffman, J. Phys. B: At., Mol. Opt. Phys. **49**, 202001 (2016).

[20] T. Wilk, A. Gaëtan, C. Evellin, J. Wolters, Y. Miroshnychenko, P. Grangier, and A. Browaeys, Phys. Rev. Lett. **104**, 010502 (2010).

[21] L. Isenhower, E. Urban, X.-L. Zhang, A. T. Gill, T. Henage, T.-A. Johnson, T.-G. Walker, and M. Saffman, Phys. Rev. Lett. **104**, 010503 (2010).

[22] H. Levine, A. Keesling, A. Omran, H. Bernien, S. Schwartz, A. S. Zibrov, M. Endres, M. Greiner, V. Vuletić, and M. D. Lukin, Phys. Rev. Lett. **121**, 123603 (2018).

[23] H. Bernien, S. Schwartz, A. Keesling, H. Levine, A. Omran, H. Pichler, S. Choi, A. S. Zibrov, M. Endres, M. Greiner *et al.*, Nature (London) **551**, 579 (2017).

[24] A. Keesling, A. Omran, H. Levine, H. Bernien, H. Pichler, S. Choi, R. Samajdar, S. Schwartz, P. Silvi, S. Sachdev *et al.*, Nature (London) **568**, 207 (2019).

[25] A. Omran, H. Levine, A. Keesling, G. Semeghini, T. T. Wang, S. Ebadi, H. Bernien, A. S. Zibrov, H. Pichler, S. Choi *et al.*, Science **365**, 570 (2019).

[26] H. Levine, A. Keesling, G. Semeghini, A. Omran, T. T. Wang, S. Ebadi, H. Bernien, M. Greiner, V. Vuletić, H. Pichler *et al.*, Phys. Rev. Lett. **123**, 170503 (2019).

[27] T. Graham, M. Kwon, B. Grinkemeyer, Z. Marra, X. Jiang, M. Lichtman, Y. Sun, M. Ebert, and M. Saffman, Phys. Rev. Lett. **123**, 230501 (2019).

[28] P. Král, I. Thanopulos, and M. Shapiro, Rev. Mod. Phys. **79**, 53 (2007).

[29] T. Pohl, T. Pattard, and J. M. Rost, Phys. Rev. A **68**, 010703(R) (2003).

[30] J.-E. Johnson and S.-L. Rolston, Phys. Rev. A **82**, 033412 (2010).

[31] J. Zeiher, R. Van Bijnen, P. Schauß, S. Hild, J.-y. Choi, T. Pohl, I. Bloch, and C. Gross, Nat. Phys. **12**, 1095 (2016).

[32] L.-I.-R. Gil, R. Mukherjee, E.-M. Bridge, M.-P.-A. Jones, and T. Pohl, Phys. Rev. Lett. **112**, 103601 (2014).

[33] M. A. Norcia, A. W. Young, W. J. Eckner, E. Oelker, J. Ye, and A. M. Kaufman, Science **366**, 93 (2019).

[34] G. Pupillo, A. Micheli, M. Boninsegni, I. Lesanovsky, and P. Zoller, Phys. Rev. Lett. **104**, 223002 (2010).

[35] A. Dauphin, M. Muller, and M.-A. Martin-Delgado, Phys. Rev. A **86**, 053618 (2012).

[36] T. Keating, C. H. Baldwin, Y.-Y. Jau, J. Lee, G. W. Biedermann, and I. H. Deutsch, Phys. Rev. Lett. **117**, 213601 (2016).

[37] Y.-Y. Jau, A. Hankin, T. Keating, I. Deutsch, and G. Biedermann, Nat. Phys. **12**, 71 (2016).

[38] J. Lee, M. J. Martin, Y.-Y. Jau, T. Keating, I. H. Deutsch, and G. W. Biedermann, Phys. Rev. A **95**, 041801(R) (2017).

[39] T. Keating, R. L. Cook, A. M. Hankin, Y.-Y. Jau, G. W. Biedermann, and I. H. Deutsch, Phys. Rev. A **91**, 012337 (2015).

[40] D. Møller, L. B. Madsen, and K. Mølmer, Phys. Rev. Lett. **100**, 170504 (2008).

[41] D. D. Bhaktavatsala Rao and K. Mølmer, Phys. Rev. A **89**, 030301(R) (2014).

[42] I. I. Beterov, M. Saffman, E. A. Yakshina, D. B. Tretyakov, V. M. Entin, S. Bergamini, E. A. Kuznetsova, and I. I. Ryabtsev, Phys. Rev. A **94**, 062307 (2016).

[43] H. Wu, X.-R. Huang, C.-S. Hu, Z.-B. Yang, and S.-B. Zheng, Phys. Rev. A **96**, 022321 (2017).

[44] I. I. Beterov, G. N. Hamzina, E. A. Yakshina, D. B. Tretyakov, V. M. Entin, and I. I. Ryabtsev, Phys. Rev. A **97**, 032701 (2018).

[45] M. Saffman, I. Beterov, A. Dalal, E. Paez, and B. Sanders, arXiv:1912.02977.

[46] K. Mølmer and A. Sørensen, Phys. Rev. Lett. **82**, 1835 (1999).

[47] A. Sørensen and K. Mølmer, Phys. Rev. Lett. **82**, 1971 (1999).

[48] D. Jaksch, J. I. Cirac, P. Zoller, S. L. Rolston, R. Côté, and M. D. Lukin, Phys. Rev. Lett. **85**, 2208 (2000).

[49] J. P. Covey, I. S. Madjarov, A. Cooper, and M. Endres, Phys. Rev. Lett. **122**, 173201 (2019).

[50] S. Saskin, J.-T. Wilson, B. Grinkemeyer, and J. D. Thompson, Phys. Rev. Lett. **122**, 143002 (2019).

[51] J. Zhang, J. Vala, S. Sastry, and K. B. Whaley, Phys. Rev. A **67**, 042313 (2003).

[52] M. J. Martin, G. Biedermann, Y.-Y. Jau, J. Lee, and I. Deutsch, *A CPHASE Gate between Rydberg-Dressed Neutral Atoms*, Technical Report (Sandia National Lab. (SNL-NM), Albuquerque, NM (United States), 2018).

[53] L. H. Pedersen, N. M. Møller, and K. Mølmer, Phys. Lett. A **367**, 47 (2007).

[54] X. L. Zhang, A. T. Gill, L. Isenhower, T. G. Walker, and M. Saffman, Phys. Rev. A **85**, 042310 (2012).

[55] T. G. Walker and M. Saffman, in *Advances in Atomic, Molecular, and Optical Physics* (Elsevier, New York, 2012), Vol. 61, pp. 81–115.

[56] S. de Léséleuc, D. Barredo, V. Lienhard, A. Browaeys, and T. Lahaye, Phys. Rev. A **97**, 053803 (2018).

[57] I.-I. Beterov, I.-I. Ryabtsev, D.-B. Tretyakov, and V.-M. Entin, Phys. Rev. A **79**, 052504 (2009).

[58] M. H. Goerz, E. J. Halperin, J. M. Aytac, C. P. Koch, and K. B. Whaley, Phys. Rev. A **90**, 032329 (2014).